



Kleinvoet: a Spatially-Distributed Temporally-Synchronised Infrasonic Recorder

HARDWARE
METAPAPER

CHRISTIAAN M. GELDENHUYS

THOMAS R. NIESLER

*Author affiliations can be found in the back matter of this article

]u[ubiquity press

ABSTRACT

We present the hardware design of a high-fidelity, low-cost infrasonic-capable (6 Hz) passive acoustic monitoring (PAM) prototype instrument. The device allows temporal synchronisation using a variety of global navigation satellite system (GNSS) constellations. This allows the recordings made by independent spatially-distributed nodes to be synchronised in time for acoustic monitoring and localisation using, for example, time difference of arrival (TDOA). Each node is capable of sampling at 24-bit resolution with a sampling frequency that is adjustable between 8 kHz and 192 kHz. Audio samples are stored locally on a microSD card, along with timestamp and location metadata.

CORRESPONDING AUTHORS:

Thomas R. Niesler

University of Stellenbosch, ZA
trn@sun.ac.za

Christiaan M. Geldenhuys

University of Stellenbosch, ZA
cmgeldenhuys@sun.ac.za

KEYWORDS:

Passive Acoustic Monitoring; Spatially-distributed Temporal-synchronisation; Wildlife Conservation; Autonomous Recording Unit; Infrasonic Recorder; Embedded Systems

TO CITE THIS ARTICLE:

Geldenhuys, CM and Niesler, TR. 2023. Kleinvoet: a Spatially-Distributed Temporally-Synchronised Infrasonic Recorder. *Journal of Open Hardware*, 7(1): 7, pp. 1–14. DOI: <https://doi.org/10.5334/joh.58>

Main design files: github.com/CMGeldenhuis/kleinvoet

Target group: researchers in the field of bioacoustics and ecology, engineers focusing on signal processing and distributed data gathering

Skills required: SMD Soldering, 3D printing (optional) and basic programming

Similar: [AudioMoth Project](#)

See section “Build Details” for more detail.

(1) OVERVIEW

INTRODUCTION

The design we present was motivated by the desire to develop a distributed acoustic sensor network for the monitoring of elephants, whose calls extend into the infrasonic spectrum and are therefore outside the range of most audio recording equipment. Since the sensors are expected to be widely spaced, an autonomous and accurate form of temporal synchronisation was also needed, which our design provides using the precise timing offered by modern GNSS systems. Furthermore, since the sensors may be exposed to harsh environmental conditions in the open, and because they are intended for use in speculative research, their cost should be low. Commercially available audio recording equipment extending into the infrasonic range is costly and does not offer temporal synchronisation between distributed sensors.

Our design is named *Kleinvoet* (“small foot” in Afrikaans), since it is the successor of a previous design, *Grootvoet* with a similar aim (Byker, 2018). It uses the TDK ICS-40300 microelectromechanical systems-based (MEMS) microphone with an acoustic frequency response characterised down to 6 Hz. For time synchronisation, the U-Blox SAM-M8Q GNSS module was chosen for its low-cost, configurable timepulse features and integrated radio frequency (RF) circuitry. The data samples are written to on-board non-volatile memory in the form of a removable memory card, though future versions may include wireless communication. Six prototype units have been built and tested in the laboratory as well as, to a limited extent, in an outside environment. The resulting measurements show that the design can continuously record stereo 24-bit audio samples with a missed sample rate less than 0.1%, using low-cost microSD cards. When fitted with a 5000 mAh Li-Ion battery, the recorders have an approximate battery life of 4.5 days when recording continuously at 24 kHz, and inserting a GNSS timestamp once every second. The fully assembled recorder with stereo infrasonic sensors costs approximately 45 USD, and an additional 40 USD for the optional weatherproof enclosure.

The structure of the remainder of the paper is as follows. First, we present an overall implementation of the design. This is followed by descriptions of the electronic hardware design and firmware implementations. Subsequently, the testing and evaluation of the recorders’ acoustic and temporal synchronisation performance are described. The manuscript concludes with a description of potential application scenarios for the hardware, information regarding the construction of a Kleinvoet recorder, and the challenges faced during the design of the hardware implementation.

OVERALL IMPLEMENTATION AND DESIGN

Kleinvoet consists of three subsystems, realised as three separate printed circuit boards (PCBs) to instil modularity. These three subsystems are: the microphone sensor board, the GNSS board and the main board.

The microphone board houses eight TDK ICS-40300 MEMS microphones with a low frequency cut-off at 6 Hz and an equivalent input noise (EIN) floor of 31dB_{SPL} . The GNSS board houses the U-Blox SAM-M8Q GNSS module, with support for concurrent GPS, Galileo and GLONASS constellations and is responsible for delivering accurate timing information. The main board consists of the ST Microelectronics STM32F446xC/E micro-controller unit (MCU), the microSD card holder and the low-noise analogue microphone pre-amplifier connected to the high-dynamic range Sigma-Delta analogue-to-digital converter (ADC). The specific MCU was chosen for its dedicated hardware peripherals that allow communication with the ADC and the microSD card.

Furthermore, the high-capacity internal memory allows more audio samples to be buffered, enabling the use of low-cost microSD cards.

Kleinvoet has been designed with a modular sensor interface to allow the future design of domain-specific sensor boards. The work presented in this manuscript, however, specifically concerns the reference design of an infrasonic-capable acoustic recorder.

Figure 1 provides an overview of the implementation of the Kleinvoet recorder. The analogue microphone signal is amplified and low-pass filtered by a set of three integrated amplifiers. The low-pass filter acts as an anti-aliasing filter and has been designed with a Bessel filter polynomial for a constant group delay in its passband. The signal is then discretised by a Sigma-Delta ADC at a configurable sampling rate ranging from 8 kHz to 192 kHz. The sampled signal is transferred and stored on the MCU of the main board, using a double-circular buffer implemented using 64 KiB volatile static random-access memory (SRAM).

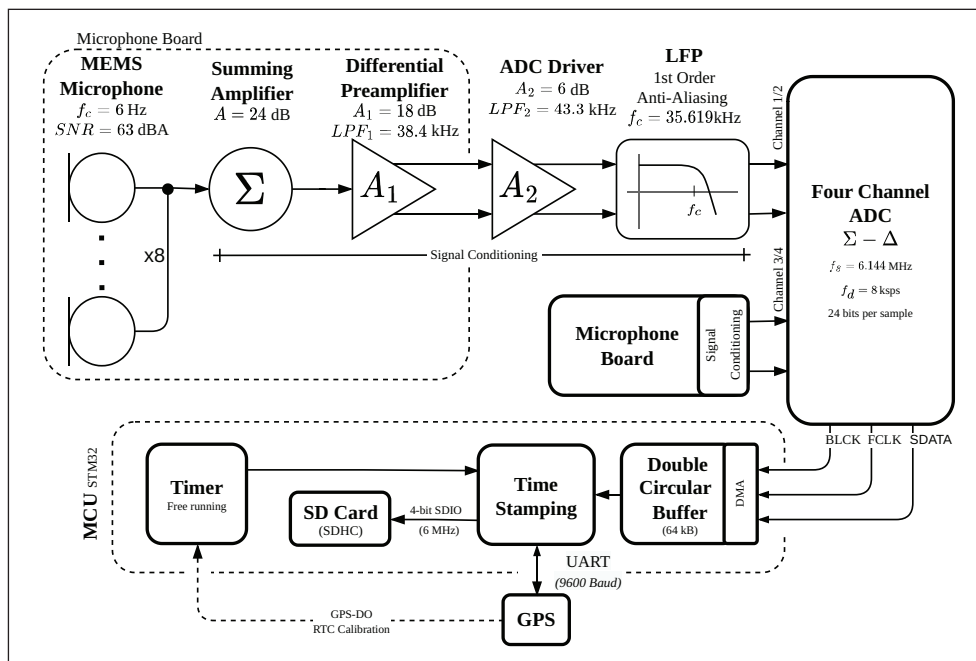


Figure 1 System diagram of a Kleinvoet recorder.

A circular buffer is a first-in first-out (FIFO) loop data structure with a fixed capacity, commonly used in data stream processing. Double buffering is a signal processing technique used where, while one buffer is being filled with data samples, the second buffer can be processed in parallel, without any race conditions. An asynchronous subroutine timestamps the recording at regular intervals before it is stored on non-volatile flash memory (removable microSD card). The timestamping information is obtained from the GNSS board via a serial UART interface and free running timer module.

Electronic Design

The eight microphone capsules are placed in a circular array (diameter of 16 mm) and are actively summed to form a single microphone with reduced self-noise and improved total harmonic distortion (THD). Since the self-noise of the individual microphones can be assumed to be statistically independent, a theoretical noise-floor improvement of 9 dB can be achieved — 3 dB for every doubling in the number of microphones (Analog Devices, 2014).

The analogue signal from the MEMS microphones is passed through a low-noise anti-aliasing low-pass filter and a gain amplification stage. The 5th order anti-aliasing filter has low pass-band noise because the noise gain and noise resonance are incorporated into the design, as presented by Steffes (2006). A total of 30 dB of gain is applied over three amplification stages to take advantage of the full input range of the external ADC for a reference acoustic signal at $94\text{ dB}_{\text{SPL}}$ and ADC dynamic range of 109 dB.

Firmware Implementation

The Kleinvoet firmware implementation is entirely written in C with minimal dependencies to allow for a high degree of portability. A basic asynchronous runtime is implemented to allow for the concurrent execution of the following tasks:

- ADC sample- and GNSS timestamp persistence
- Operational log management
- User interface and read-eval-print loop (REPL) handling
- System health monitoring, such as GNSS uplink, battery status and MCU temperature.

Timestamping is handled asynchronously with the use of a free-running hardware timer and a high-priority interrupt. The free running hardware timer is connected to the *frame sync* signal of the ADC and the *time pulse* signal of the GNSS module. The GNSS module is configured to output one pulse every second (1 Hz). At the start of each new sample frame — equal to the sampling frequency — the *frame sync* signal changes polarity, which increments the counter register of the hardware timer. By employing dedicated hardware for this task, a reliable frame count is ensured. The GNSS module then transmits the timestamp metadata associated with the previous time pulse over a universal asynchronous receiver-transmitter (UART) interface. This metadata, along with the associated frame index, is stored, allowing for the recordings made by separate recorders to be synchronised. This allows the generation of timestamp information to within half a sampling period accuracy, synchronised with the coordinated universal time (UTC) standard obtained from the chosen GNSS satellite constellation.

The recordings are split into 256 MiB pulse-code modulation (PCM) WAV files. The associated estimate for both time and location with the lowest error, as reported by the GNSS module, are stored in the file header metadata. If verbose timestamps are required, each decoded timestamp along with the respective frame count is stored as a CSV file along with the recording.

Weatherproofing and Enclosure

Optionally, Kleinvoet can be placed in a weatherproof enclosure with additional wind filtering and liquid ingress prevention. The wind filters are suited for gusts of wind. In the presence of a persistent speed, additional wind filtering material is recommended. The addition of a weatherproof enclosure and wind filtering makes Kleinvoet ideally suited for long-running outdoor experiments. However, it should be noted that the addition of an enclosure and wind filters does impact the overall frequency response. A set of 3D-printed adaptors are required to mount the PCBs in the recommend enclosure. If used without an enclosure, a 3D printer is not required by the design. If an enclosure is not required, the PCBs have been designed to snap together into a cube, held together by rubber bands or cable ties.

(2) QUALITY CONTROL

SAFETY

As lithium-based batteries are used, the usual precautionary measures should be taken.

All electronic components are RoHS compliant and can be assembled with lead-free solder.

When assembling the recorders, ensure that the devices are not powered, as this can cause permanent damage to the components. During the connection of internal PCB interconnects, ensure that the assembler is sufficiently grounded, as some internal components have minimal electrostatic discharge (ESD) protection. The microSD card holder and USB-C port include sufficient ESD protection for ungrounded user operation.

GENERAL TESTING

To ensure the recorders perform as expected, the recorders have been assessed in terms of frequency response, synchronisation accuracy and weatherproofing. Furthermore, the recorders have been used in a preliminary data gathering excursion, where the nodes were exposed to the expected field conditions.

Magnitude spectral estimate

To characterise the acoustic performance of a Kleinvoet recorder, the frequency response was estimated using the techniques described in Welch (1967), Vold, Crowley, and Rocklin (1984), and Bendat (2010). To reduce measurement error due to external noise factors, all acoustic measurements were taken in an acoustically damped recording studio. A test excitation signal was played through a set of reference loudspeakers (KRK ROKIT 10s and KRK ROKIT 8) and simultaneously recorded by a reference microphone (Sennheiser MKH 8020) and a Kleinvoet recorder. A 30 second Gaussian white noise signal was chosen as the excitation signal. This method of measurement is known as a two port measurement (Hayes, 1996). Figure 2, shows a Kleinvoet node in a two port test setup with a reference microphone as the input port and the Kleinvoet recording as the output.

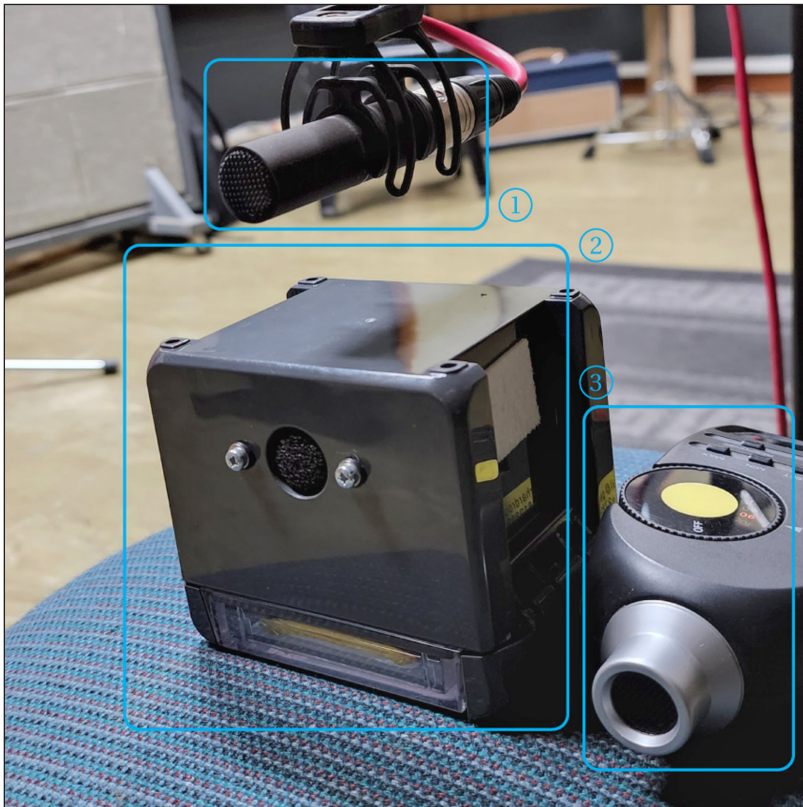


Figure 2 Photograph of recording set up, for Kleinvoet frequency response estimation. Depicted is ①: Sennheiser MKH 8020 reference microphone, ②: Kleinvoet and ③: calibrated sound pressure level (SPL) meter. Conducted in an acoustically damped recording studio.

Figure 3 shows the magnitude spectral response estimate for a Kleinvoet recorder using the method described above. The response estimate shows that Kleinvoet features a linear response from 40 Hz to 400 Hz, which is also the band of interest for elephant rumbles (Wood et al., 2005). The resonant peak around 700 Hz is a known artefact of the ICS-40300 MEMS microphone. Unfortunately, generating low-frequency acoustic signals has proven to be difficult, as most acoustic hardware includes electronic filtering that removes frequency components below 20 Hz (Walker et al., 2008). This is the reason for the sudden decrease in coherence below 30 Hz. As a single loudspeaker did not extend over a wide enough frequency range, two loudspeakers were used as an excitation source instead. The cross-over point was set to 70 Hz and is the cause of the reduction in coherence at this frequency. The slight drop in coherence at 50 Hz and 100 Hz is due to the interference from the 50 Hz electrical grid power grid in South Africa. The reduced coherence near 200 Hz, 500 Hz and 800 Hz are believed to be artefacts of the acoustically damped room.

Synchronisation Accuracy

This section will consider the accuracy with which recordings, made by independent nodes¹ can be synchronised using the integrated GNSS timestamp information.

¹ The term “node” is used here rather than “recorder” to signify that a device forms part of a sensor network, rather than just a single recording device.

When no post-processing is used, the maximum synchronisation error is equal to half the sample period ($\frac{t_s}{2}$). In this case, the dominating factor determining synchronisation is the discrete alignment of the independently recorded signals. However, the GNSS module is capable of delivering more precise timing information than the resolution dictated by the sampling rate. Temporal synchronisation errors resulting from GNSS related timing errors and/or temporal alignment errors result in a constant bias in the resulting localisation error, while synchronisation drift, caused by oscillator drift, will result in the localisation error to drift over time (El Gemayel, Jäkel, and Jondral, 2014; Díez-Gonzalez, Sánchez-González, Perez, et al., 2020).

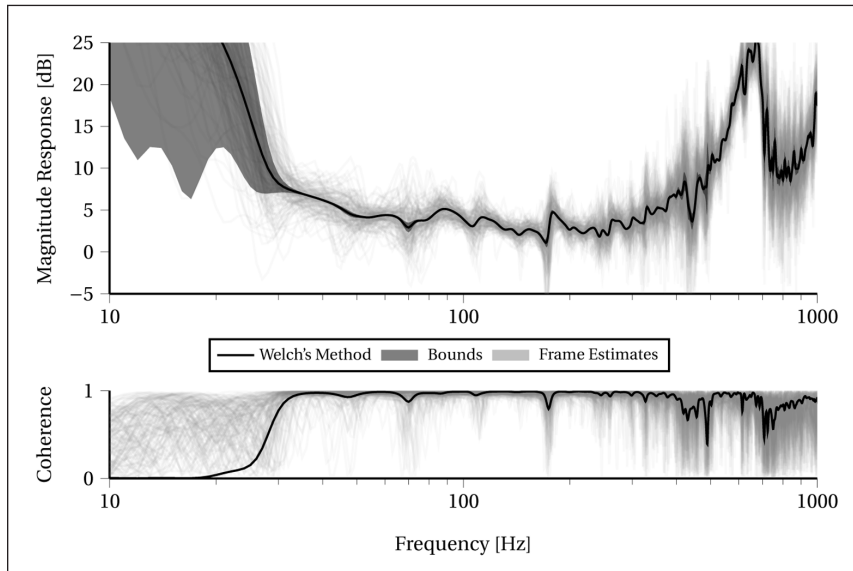
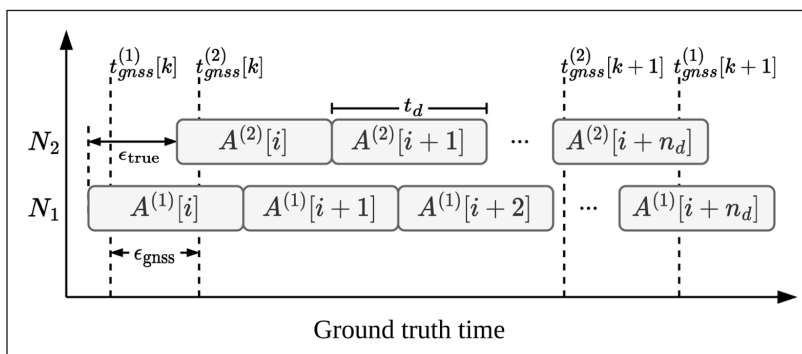


Figure 3 Magnitude spectral response estimate for a Kleinvoet recorder sampling at 48 kHz and assembled in a weatherproof case fitted with a wind filter. Periodograms are computed from 12000 sample long that overlap by 50%. A Blackmann data window is applied after zero-padding to 48000 samples. Welch's method for spectral averaging is applied across all periodograms, to obtain a reduced variance frequency response estimate. The coherence indicates the degree of uncorrelated noise sources present in the estimation process.

To evaluate the device's synchronisation error, two nodes were set up in an open area away from buildings, as the synchronisation error has been observed² to be dependent on the GNSS reception strength (Drinic and Marshall, 2008). The nodes were configured to record for 10.5 hours, with a timestamp logged once per second. Ideally, the two nodes will estimate and report the exact same timestamp information. However, due to the way in which GNSS receivers estimate timing information, these two timestamps are rarely exactly the same, differing by an error term ϵ_{gnss} . Figure 4 illustrates the difference in timestamps between two independently sampling nodes, comparing the timing errors present during the process of temporal synchronisation. Figure 5 shows a histogram of the measured synchronisation error, ϵ_{gnss} . The gathered data has an root mean square error (RMSE) of 302.329 ns and a standard deviation of 30.414 ns. In comparison, at the highest sampling rate (192 kHz), the synchronisation error ($\frac{t_s}{2}$) is 2604.167 ns and at the lowest it is 62 500 ns. As the synchronisation error introduced by the alignment of the discrete samples is much larger than the GNSS timing error ϵ_{gnss} , we see that the discrete sampling rate remains the dominant source of temporal synchronisation and alignment accuracy. In future work, other methods of synchronisation can be explored, such as upsampling or fractional delay filters, to improve the achieved alignment to within an error dictated by the GNSS reference, rather than the sampling frequency.

Figure 4 An illustration, not to scale, of the temporal synchronisation errors arising between two recording nodes, N_1 and N_2 . The ADC sample interval is indicated as t_{gr} , and two almost simultaneous samples at discrete time i by $A^{(1)}[i]$ and $A^{(2)}[i]$ for nodes N_1 and N_2 , respectively. Nodes N_1 and N_2 also receive GNSS-triggered timestamps (derived from the *TIMEPULSE* signal) to mark these samples. The k_{th} discrete timestamps are denoted $t_{gnss}^{(1)}[k]$ and $t_{gnss}^{(2)}[k]$. Due to the small error in decoding the *TIMEPULSE* signal at each node, these two timestamps, which should ideally be simultaneous, are in fact ϵ_{gnss} seconds apart. However, timestamps are associated with the most recent sample. Therefore, the true time misalignment between the two samples is in fact ϵ_{true} .



² Informal experimentation has shown that a weak GNSS signal can lead to an 12-18 fold increase in error of the GNSS time pulse generation and timestamp reporting.

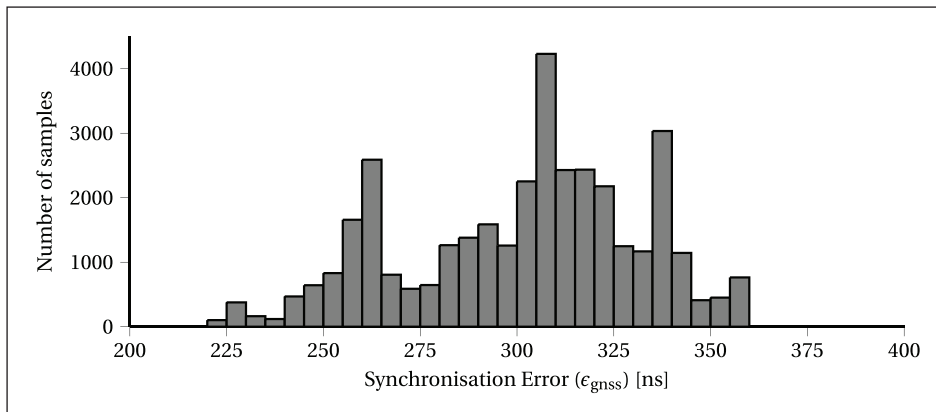


Figure 5 Histogram showing the measured synchronisation error between two nodes in nanoseconds when GNSS timestamp are captured once per second, for a duration of 10.5 hours.

Field data gathering

The hardware has undergone two field tests in the South African bushveld. Five recorders were deployed for a period of one week at a wildlife reserve near Rustenburg, South Africa. A second dataset using four recorders was collected, over a similar period near Bela-Bela, South Africa. A total of 160 GB worth of recordings were collected, with a total recording time of 80 hours. [Figure 6](#), shows a Kleinvoet recording node deployed in the South African bushveld.



Figure 6 Kleinvoet deployed in South Africa, during a data gathering excursion.

During both field dataset collection excursions, the recorders were exposed to weather conditions that included strong rain, thunderstorms, direct ultra-violet (UV) exposure and high ambient temperatures (approximately 38°C). Although the field tests are limited, the recorders remained intact and fully operational.

During high ambient temperatures (>35°C) and direct exposure to the sun for prolonged periods (>6 h), one recorder would occasionally halt operation for 30 seconds due to overheating. In this event, the recorder's watchdog timer was triggered, and the device reset to allow for self-recovery. This has happened on only one occasion, and when the recorder was placed in direct sunlight.

Weatherproofing

The Kleinvoet recorders were evaluated in terms of weatherproofing by artificially subjecting one fully assembled unit to the following tests:

1. Water spray from directly above for 1 hour.³
2. Water spray at a angle of 45 degrees to the microphone inlet port, for 30 minutes.
3. Water spray perpendicular to the side of the case, directly at the microphone port, for 30 minutes.
4. Device fully submerged (10 cm) for 30 minutes.

³ All water-related tests were performed outside to reduce water wastage.

To evaluate whether any water was able to enter the enclosure, a set of relative humidity and liquid reactive test indicator cards was used. These cards react to the presence of liquid or an increase in humidity, with indicators for 5%, 10%, and 60% humidity levels. During all water spray tests, a test card was kept outside the enclosure in the same environment but away from the water jet, to serve as a control. As stated in the assembly and usage guide in the software repository,⁴ the wind filter also serves as a weatherproofing seal, and should be replaced after each complete disassembly of the recorder. Furthermore, the results presented in this section are preliminary as they were not conducted by a certified ingress protection (IP) laboratory.

In all tests, only the 5% indicator tested positive. However, for the control card, both the 5% and 10% indicators were triggered, indicating a higher humidity outside the enclosure than inside.

Both the artificial water ingress tests and the practical real-world field tests found that in no case did any water enter the enclosure. Furthermore, the internal humidity levels remained unaffected by the water jet and the submersion tests. We therefore conclude that the enclosure and weather sealing used in the Kleinvoet design is adequate to prevent water ingress, and that the recorders are sufficiently weatherproof for data collection purposes for the expected field conditions.

(3) APPLICATION

USE CASE(S)

Distributed offline localisation

In this section, we demonstrate the feasibility of passive acoustic source localisation using recordings made by a set of Kleinvoet recorders. We will consider only one prevalent localisation algorithm, named *hyperbolic multilaterisation* (Marchand, 1964; Lee, 1975). In particular, the *trilaterisation* (Fang, 1986) variant for the case of three sensor nodes is chosen. The non-linear hyperbolic multilaterisation loss function for a single recording node n is given by the following equation:

$$\mathcal{L}_n(\vec{s}) = \left| \|\vec{s} - \vec{p}_n\| - \|\vec{s} - \vec{p}_0\| - \tau_n \cdot c \right| \quad (1)$$

where \vec{s} is the set of co-ordinates indicating the position of the unknown sound source, \vec{p}_n is the position of n^{th} node, \vec{p}_0 is the position of the reference node with respect to which the TDOA τ_n is computed, c is the wave speed of sound and $\|\cdot\|$ is the Euclidean distance. The sum of the loss function over all three recording nodes is minimised with respect to the estimated sound source location using a numerical optimisation technique known as the *interior point line search filter method* (Waltz et al., 2006).

Recordings were collected using three recorders during early development of the project. These recordings were taken on the rooftop of a building located at the Electrical and Electronic Engineering Department of Stellenbosch University. Table 1 provides a summary of the data collected in this section.

	LOCATION 1	LOCATION 2	LOCATION 3
Length of Recording	11.62 min	10.87 min	9.54 min
Repeated Rumbles	3	3	3
Wind Present	Yes	No	No
Number of Recorders	3	3	3
Inside Perimeter	Yes	Yes	Yes
Sample Rate	16 kHz	16 kHz	16 kHz

Table 1 Summary of the data gathered on rooftop located on the Electrical and Electronic Engineering Department of Stellenbosch University. Location 1, -2 and -3 refer to the three sound source locations tested.

4 github.com/CMGeldenhuys/kleinvoet.

Three recorders were placed in a 10 m × 15 m right-angled triangular arrangement. A sound source was placed inside the triangular perimeter formed by the three recorder locations as vertices. A recording of an African elephant rumble was reproduced using a loudspeaker (sound source), noting the exact location of the source relative to the position of the recording nodes. Each recording consisted of three identical rumbles in quick succession, each with a duration of approximately two and a half seconds. The loudspeaker was stationary during each recording. A 5 minute period of ambient recording (no elephant rumble sound emission), was included at the start and the end of each recording. A total of three recordings were made in this way, with three different sound source locations.

First, the approximately 10 minute long recordings made by each of the distributed nodes (Table 1) were temporally synchronised to the nearest sample using the accompanying periodic timestamp metadata. The silences were then removed from the start and the end of the recordings, keeping only the recording of the sound source. The truncated recordings were then segmented into overlapping frames, the size of which is discussed later in this section. A Blackman spectral window was applied to each frame before estimating the TDOA by computing the peak in the general cross-correlation between a recording node and a chosen reference node (Havelock, Kuwano, and Vorländer, 2008). From these estimated TDOA values and the GNSS positional metadata for each recorder, the location of the sound source could be estimated using hyperbolic multilateration for each audio frame. Note, however, that although there may in practice be multiple sound sources in a given frame, the above technique only computes a single location estimate per frame.

The cross-correlation, required for the TDOA computation, was computed using a fast Fourier transform-based (FFT) method with a frame size of 16384 samples (approx. 680 ms), and an inter-frame overlap of 50% (8192 samples, approx. 340 ms). The length of the frame determines the largest TDOA that can be estimated, and was chosen based on the time it would take an acoustic signal to propagate between the two furthest nodes. Since in this experiment we have confined the sound source to lie within the perimeter of the nodes, this is a safe assumption to make. However, in practice a different frame length may be chosen.

The computed RMSE between each localisation estimate and the ground truth location of the sound source, was found to be 2.8 m and 1.6 m in the x- and y-directions, respectively, while the overall RMSE was 3.2 m. Figure 7 shows all the localisation estimates (rendered with a 10% opacity) and the ground truth localisation. Due to the high density of the localisation estimates, the estimate appears opaque. The sparse (low density) localisation estimates surrounding the ground truth correspond to frames with low energy or frames at the start of the rumble, where the signal (rumble) is not yet perceivable by all the recorders.

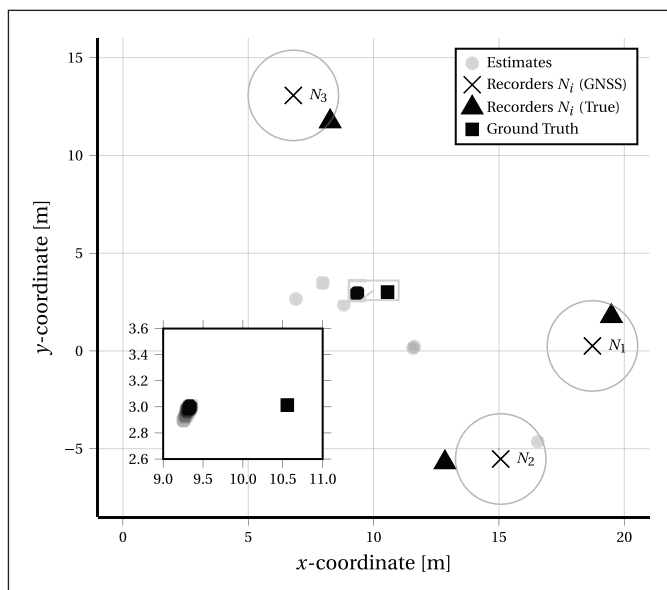


Figure 7 Hyperbolic multilateration localisation using TDOA with three Kleinvoet recorders regularly spaced around a sound emission source. Shown are the localisation estimates for a short (16384) frame length and GNSS provided recorder locations. The inset shown in the bottom left of the figure shows 72 localisation estimates (total of 165) near the ground truth in greater detail.

The nodes have a known positional error, shown in Figure 7 by a circle around the positional marker. This error is a limitation of using GNSS modules to determine the recorders' location.

Future work could improve on this error by considering the node's location as a time-series of estimates while the nodes remains stationary. A second source of error is the geodesic coordinate system, which has a known degree of accuracy. The coordinates provided by the GNSS module are in the global Earthcentred Earth-fixed (ECEF) spherical coordinate system (WG84 ellipsoid). This coordinate system has a maximum accuracy of 2 m. If we correct the node position estimates, as reported by the GNSS module, to the known distributed array geometry, the RMSE error reduces to 1.3 m (1 m and 0.9 m in the x- and y-directions, respectively).

The localisation results for the above section are summarised in Table 2. These results demonstrate that a set of recordings made using Kleinvoet recorders can be used to successfully localise acoustic sources using TDOA hyperbolic multilateration.

FRAME LENGTH	RECORDER POSITION	RMSE		
		X	Y	COMBINED
Short (16384)	GNSS	2.776 m	1.571 m	3.190 m
Short (16384)	Ground Truth	1.264 m	1.679 m	2.102 m
Long (61440)	GNSS	1.477 m	0.983 m	1.774 m
Long (61440)	Ground Truth	1.001 m	0.874 m	1.329 m

Table 2 Summary of root mean square error (RMSE) for localisation results, using recordings taken with Kleinvoet recorders, illustrating the effects of different frame lengths and GNSS position error.

REUSE POTENTIAL AND ADAPTABILITY

Both the hardware and firmware of the Kleinvoet project are open-source, making the project versatile. Certain parts of Kleinvoet were designed to be modular, such as the sensor connection, allowing one to use the base recorder design with a custom set of sensors, other than microphones. The sensor interface has been designed to be electrically compatible with professional and consumer audio equipment. However, due to the wide range of equipment available, strict compatibility cannot be guaranteed and was only tested on a small subset of third-party devices. As there is no common industry standard connector for geophones, hydrophones, microphones or arbitrary analogue sensors, an adaptor board will have to be designed to integrate such sensors with the main system.

Although the system has been designed with the intent of elephant monitoring, the recorder offers a wide range of sampling frequencies and the reference sensor board's acoustic characterisation extends beyond the band of interest for elephant vocalisations. As such, the recorders could be used for general-purpose outdoor recordings and passive acoustic monitoring (PAM) of other animal species that communicate in the band 6 Hz to 40 kHz.

(4) BUILD DETAILS

AVAILABILITY OF MATERIALS AND METHODS

In order to manufacture a Kleinvoet recorder, it is necessary to source the individual electronic- and integrated circuits (ICs) components. These were all readily available during the design of Kleinvoet from several well-known and reputable suppliers.

The Kleinvoet design includes three 4-layer PCBs. Since all RF functionality is integrated into discrete modules, there are no stringent constraints regarding the PCB fabrication. The tolerances have been kept low to allow for easy PCB fabrication. Although a 4-layer PCB is typically used in RF work, the use of it here is justified by the desire for low-noise performance. In order to allow the full dynamic range of the 24-bit ADC to be used, special care had to be taken to ensure that minimal electrical noise is contributed by the analogue signal chain and accompanying digital electronics. To ensure sufficient mitigation of cross-talk between the sensitive analogue circuitry and switching digital circuitry, the respective circuits are kept as far away from each other as possible. Furthermore, a solid ground reference plane was used in close proximity to sensitive PCB signal traces. The inner two layers of the PCB are dedicated reference planes.

When using the recommended, but optional, weatherproofing enclosure, a 3D printer is required to print adaptor plates for the PCB. The adaptor plates have no overhangs and can be printed using an entry level 3D printer without additional tuning.

EASE OF BUILD

Figure 8 shows an exploded disassembly view of the complete Kleinvoet construction, indicating the three PCBs namely: the main board (3), the GNSS board (4) and the microphone sensor board (6). Assembly of the Kleinvoet PCBs requires the use of hot-air reflow soldering. It is recommended that a professional assembly service be contacted to assemble the boards.

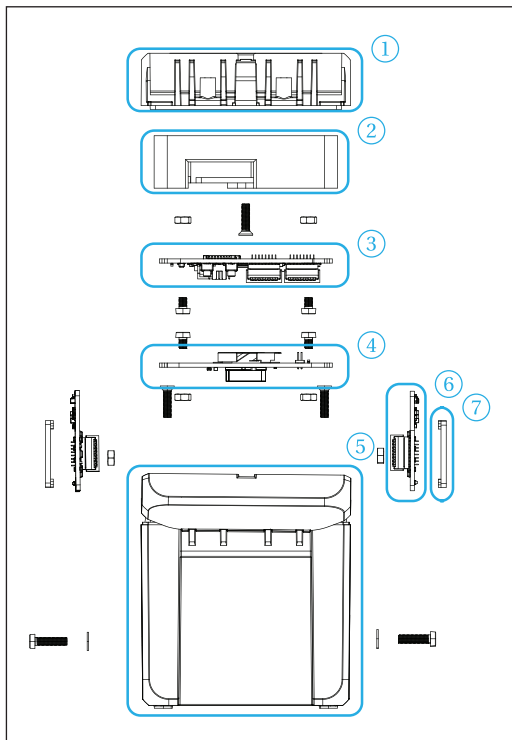


Figure 8 Exploded disassembly schematic of Kleinvoet construction, showing: ①: Enclosure lid, ②: 3D-printed main board adaptor, ③: Main PCB, ④: GNSS PCB, ⑤: Enclosure base, ⑥: Microphone sensor PCB and ⑦: 3D-printed sensor spacer.

However, Kleinvoet has been designed in such a way that most components are placed on the same side of the PCB. This allows for hot-plate or oven-based reflow soldering, or automated pick-and-place assembly, leaving only two large components (microSD card holder and optional real-time clock (RTC) battery holder) to be soldered manually. This method of assembly has however not been tested.

OPERATING SOFTWARE AND PERIPHERALS

An ST-Link or JTAG equivalent programming probe is required to flash the initial firmware to the internal flash memory. These probes are inexpensive and easily obtainable. Only one probe is required and can be used to program several Kleinvoet recording nodes.

After the firmware has been flashed to the device, it is fully self-contained and self-configuring. The nodes require no external software or peripherals to operate. Once the device is powered, it will self-configure and start to record, according to its schedule. Kleinvoet has an integrated Lithium battery charger. The charger is powered by the USB-C port on the device.

DEPENDENCIES

The Kleinvoet firmware depends on the STM32 hardware abstraction layer (HAL) library, the *FatFS* library by Chan and the *fifofast* library by Nqtronix. The HAL libraries are open source and distributed under the 3-clause BSD license BSD license (ST Microelectronics, 2021). The external library *FatFS* are open-source and distributed under the 1-clause BSD license (Chan, 2021). Finally, the *fifofast* library is open-sourced under the MIT license (Nqtronix, 2019).

Name: Kleinvoet hardware design files

Persistent identifier: [10.5281/zenodo.7816492](https://doi.org/10.5281/zenodo.7816492)

Licence: Strongly-reciprocal CERN Open Hardware Licensing version 2 (CERN-OHL-S)

Publisher: Zenodo

Date published: 27/03/2023

Name: Kleinvoet firmware

Persistent identifier: [10.5281/zenodo.7816498](https://doi.org/10.5281/zenodo.7816498)

Licence: GNU General Public License version 3 (GNU GPLv3)

Publisher: Zenodo

Date published: 27/03/2023

(5) DISCUSSION

CONCLUSION

We have presented Kleinvoet, an open-source design for an automated recording unit. Kleinvoet recorders sample at 24-bit resolution, with a configurable sampling rate ranging from 8 kHz to 192kHz. The design offers the key feature of GNSS-based temporal synchronisation to within half a sample period. This can be improved by additional post-processing. This allows recordings made by multiple individual recorders to be synchronised in time, as required for distributed localisation experiments. The recorder can be extended by the addition of modular sensor boards, and offers an infrasonic-capable microphone as part of the design. The recorders have been tested in both a laboratory setting and a field environment. Furthermore, it has been demonstrated in preliminary experiments that recordings made with the Kleinvoet recorders can be successfully used to perform passive acoustic sound source localisation by TDOA multilateration. The recorders are actively being used as part of ongoing research in the field of infrasonic localisation.

FUTURE WORK

Future improvements to the platform could include the addition of a short range wireless communication to allow local monitoring of the device. Improvements to the low-frequency noise floor by using a medium or large diaphragm condenser microphone element in combination with a MEMS array are also a possibility. Improved power conversion and battery charge monitoring would allow improved battery life. Finally, additional microSD card holders could be added to allow for longer recording duration.

The assembling MEMS based microphones can be difficult using hot-air soldering. This is due to the capsules requiring specific heat reflow temperature curves. The capsules can become damaged if flux or solder is drawn into the microphone capsule inlet port, through the capillary effect. Improvements to the microphone PCB may allow for easier assembly using oven-based reflow soldering, reducing the chances of damage occurring to the capsules during assembly.

ACKNOWLEDGEMENTS

We acknowledge the fine-mechanical technical team and workshop of the Department of Electrical and Electronic Engineering, Stellenbosch University for their invaluable assistance in manufacturing a set of prototype devices.

FUNDING INFORMATION

The hardware development, production cost and ongoing research is funded by the Digital Signal Processing Laboratory at the University of Stellenbosch.


The authors have no competing interests to declare.

AUTHOR CONTRIBUTIONS

The initial idea was proposed by TRN. CMG was responsible for the hardware design, firmware development and testing of the Kleinvoet recorders. All authors contributed equally to the creation and review of the manuscript, along with compiling the file repositories.

AUTHOR AFFILIATIONS

Christiaan M. Geldenhuys  orcid.org/0000-0003-0691-0235
University of Stellenbosch, ZA

Thomas R. Niesler  orcid.org/0000-0002-7341-1017
University of Stellenbosch, ZA

REFERENCES

- Analog Devices**, 2014. *High performance, low noise studio microphone with MEMS microphones, analog beamforming, and power management* [Online]. Application note AN-1328. Analog Devices. Available from: <https://www.analog.com/media/en/technical-documentation/application-notes/an-1328.pdf>.
- Bendat, J.S.**, 2010. *Random data: analysis and measurement procedures*. 4th ed., Wiley series in probability and statistics. Hoboken, NJ: Wiley. DOI: <https://doi.org/10.1002/9781118032428>
- Byker, R.W.**, 2018. *Infrasoniese, GPS-gesinkroniseerde klankopnemers vir die opsporing van olifantdreungeluide* [Online]. Master's Thesis. University of Stellenbosch. Available from: <http://hdl.handle.net/10019.1/104999>.
- Chan, N.**, 2021. *FatFs – generic FAT filesystem module (v.R0.12c)* [Online]. Available from: http://elm-chan.org/fsw/ff/00index_e.html.
- Díez-Gonzalez, J., Sánchez-González, L., Perez, H.**, et al., 2020. Combined noise and clock crlb error model for the optimization of node location in time positioning systems. *IEEE access* [Online], 8, pp. 31910–31919. DOI: <https://doi.org/10.1109/ACCESS.2020.2973709>
- Drinic, D. and Marshall, C.**, 2008. *Accurate timing for the IoT*. (whitepaper). U-blox.
- El Gemayel, N., Jäkel, H., and Jondral, F.K.**, 2014. Error analysis of a low cost TDoA sensor network. 2014 *IEEE/ION position, location and navigation symposium – PLANS 2014* [Online]. IEEE, pp. 1040–1045. DOI: <https://doi.org/10.1109/PLANS.2014.6851484>
- Fang, B.T.**, 1986. Trilateration and extension to global positioning system navigation. *Journal of guidance, control, and dynamics* [Online], 9(6), pp. 715–717. DOI: <https://doi.org/10.2514/3.20169>
- Havelock, D., Kuwano, S., and Vorlander, M.**, (eds.), 2008. *Handbook of signal processing in acoustics*. Springer. DOI: <https://doi.org/10.1007/978-0-387-30441-0>
- Hayes, M.H.**, 1996. *Statistical digital signal processing and modeling*. New York: John Wiley & Sons.
- Lee, H.B.**, 1975. A novel procedure for assessing the accuracy of hyperbolic multilateration systems. *IEEE transactions on aerospace and electronic systems*, (1), pp. 2–15. DOI: <https://doi.org/10.1109/TAES.1975.308023>
- Marchand, N.**, 1964. Error distributions of best estimate of position from multiple time difference hyperbolic networks. *IEEE transactions on aerospace and navigational electronics*, (2), pp. 96–100. DOI: <https://doi.org/10.1109/TANE.1964.4502170>
- Nqtronix**, 2019. *Fifofast – a fast, generic FIFO for MCUs (v.0.8.0)* [Online]. Available from: <https://github.com/nqtronix/fifofast>.
- ST Microelectronics**, 2021. *Description of STM32F4 HAL and low-layer drivers* [Online]. Application note UM1725. ST Microelectronics. Available from: https://www.st.com/resource/en/user_manual/um1725-description-of-stm32f4-hal-andlowlayer-drivers-stmicroelectronics.pdf.
- Steffes, M.**, 2006. *Design methodology for MFB filters in ADC interface applications*. Application note SBOA114. Texas Instruments.
- Vold, H., Crowley, J., and Rocklin, G.T.**, 1984. New ways of estimating frequency response functions. *Sound & vibration*, 18(11), pp. 34–38.
- Waltz, R.A., Morales, J.L., Nocedal, J., and Orban, D.**, 2006. An interior algorithm for nonlinear optimization that combines line search and trust region steps. *Mathematical programming*, 107(3), pp. 391–408. DOI: <https://doi.org/10.1007/s10107-004-0560-5>
- Walker, K., Dzieciuch, M., Zumberge, M., and DeWolf, S.**, 2008. *A portable infrasonic sensor calibrator down to at least 8 Hz*. (technical report ADA516202). Jolla Institute of Geophysics and Planetary Physics, University of California.

- Welch, P.**, 1967. The use of fast fourier transform for the estimation of power spectra: a method based on time averaging over short, modified periodograms. *IEEE transactions on audio and electroacoustics* [Online], 15(2), pp. 70–73. DOI: <https://doi.org/10.1109/TAU.1967.1161901>
- Wood**, et al., 2005. Classification of african elephant *loxodonta africana* rumbles using acoustic parameters and cluster analysis. *Bioacoustics*, 15(2), pp. 143–161. DOI: <https://doi.org/10.1080/09524622.2005.9753544>

TO CITE THIS ARTICLE:

Geldenhuis, CM and Niesler, TR. 2023. Kleinvoet: a Spatially-Distributed Temporally-Synchronised Infrasonic Recorder. *Journal of Open Hardware*, 7(1): 7, pp. 1–14. DOI: <https://doi.org/10.5334/joh.58>

Submitted: 27 March 2023

Accepted: 28 July 2023

Published: 18 August 2023

COPYRIGHT:

© 2023 The Author(s). This is an open-access article distributed under the terms of the Creative Commons Attribution 4.0 International License (CC-BY 4.0), which permits unrestricted use, distribution, and reproduction in any medium, provided the original author and source are credited. See <http://creativecommons.org/licenses/by/4.0/>.

Journal of Open Hardware is a peer-reviewed open access journal published by Ubiquity Press.